

Unified Performance Analysis of Near and Far User in Downlink NOMA System over $\eta - \mu$ Fading Channel

Shaika Mukhtar, and Gh. Rasool Begh

Original scientific article

Abstract—The non-orthogonal multiple access (NOMA) scheme is considered as a frontier technology to cater the requirements of 5G and beyond 5G (B5G) communication systems. To fully exploit the essence of NOMA, it is very important to explore the behavior of NOMA users over the most realistic non-homogenous fading conditions. In this paper, we derive unified closed-form expressions of the basic performance metrics of the NOMA users. Their performance is evaluated in terms of average bit error rate (ABER), average channel capacity (ACC) and outage probability (OP) over $\eta - \mu$ fading channel. These expressions are in terms of popular functions, such as Meijer G -function and Gauss hypergeometric function, leading to their versatile use in analytical research. Unlike the existing outage probability expressions in terms of Yacoub integral, the derived expressions are easier to implement in software packages like MATLAB. Moreover, we compare the obtained results with a reference system, consisting of genie-aided NOMA system. We interpret that genie-aided performance results provide benchmark bounds for the metrics. Extensive simulations are carried out to validate the derived analytical expressions.

Index Terms—Average bit error rate, average channel capacity, non-homogenous fading, non-orthogonal multiple access, outage probability.

I. INTRODUCTION

THE 5G communication network is expected to support massive number of high-speed users communicating with each other seamlessly. Such transmission demands a highly evolved multiple access technique that can satisfy the diverse needs of the users. In this regard, non-orthogonal multiple access (NOMA) is considered as an effective technique which allows multiple users to share the same resource block efficiently [1]. This approach ensures mass connectivity along with fairness among users. Superposition coding at transmitter and successive interference cancellation (SIC) at the receiver are the two prominent processes involved in a NOMA system. This scheme is superior to traditional orthogonal multiple access (OMA) as it offers higher data rate, better spectral efficiency and improved system performance [2], [3]. These advantages encourage the interplay of NOMA with different wireless technologies showing the flexibility and versatility of NOMA scheme [4], [5].

Manuscript received April 26, 2021; revised July 7, 2021. Date of publication October 22, 2021. Date of current version October 22, 2021.

Authors are with the Advanced Communication Lab, Department of Electronics and Communication Engineering, National Institute of Technology Srinagar, India (e-mails: shaika.mukhtar@yahoo.com, grbegh@nitsri.ac.in).

Digital Object Identifier (DOI): 10.24138/jcomss-2021-0090

The promising nature of NOMA has attracted a lot of attention from the researchers. The authors in [6] have discussed the possibilities and obstacles of NOMA for 5G networks. In [7], a practical form of NOMA known as multiuser superposition transmission (MUST) is considered for downlink transmission. Moreover, the various technical aspects of NOMA have been widely discussed. In [8] and [9], the authors have analyzed different modulation techniques for improving the performance of NOMA system. In [10], the authors have shown that NOMA has superior energy efficiency performance in comparison with conventional orthogonal multiple access. In [11], the authors have shown that outage performance of randomly deployed NOMA users depends critically on the choices of the users' targeted data rates and allocated power. Owing to the flexible nature of NOMA, the incorporation of NOMA in different technologies is comprehensively studied. In [12], the performance of NOMA is examined in terms of system throughput for uncoordinated transmissions. In [13], NOMA scheme is investigated for irregular repetition slotted ALOHA (IRSA) wherein improvement in packet loss rate (PLR) performance is obtained. In [14], the authors have analyzed the joint adoption of NOMA and repetition-based strategies under affordable energy constraints for better system performance. In addition to this, NOMA-based hybrid satellite terrestrial relay system has been examined in [15], wherein it is shown that the inclusion of NOMA improves the outage probability of the hybrid system. In [16], the authors have examined the NOMA-aided satellite communication over shadowed Rician fading channel.

In [17], NOMA has been considered for massive multiple input multiple output (mMIMO) low earth orbit (LEO) satellite communication system to improve spectral efficiency. In [18], the performance of cognitive satellite-terrestrial network is analyzed wherein closed-form expressions for the outage probability of primary satellite network and secondary terrestrial network are obtained. In [19], NOMA-aided unmanned aerial vehicle (UAV) system is analyzed as a promising solution to address spectrum scarcity problem in UAV communications. In [20], average bit rate and ergodic capacity for NOMA-aided under-water communication are derived. As evident from the open research literature, the multifaceted utility of NOMA makes it imperative to study the behavior of NOMA users in the realistic 5G non-line-of-sight (NLOS) fading environments. As such, there are various generalized fading models

which are used to characterize these hostile environments. Among these, $\eta - \mu$ fading model is the general model which encompasses the practical non-homogenous propagation mediums. The $\eta - \mu$ fading model generates special cases of fading for different values of parameters η and μ . These special cases are Nakagami- q , Nakagami- m , Rayleigh and one-sided Gaussian distributed fading channels [21]. All these fading scenarios affect the NOMA users differently. So, analyzing their performance in such fading channels helps in improving the performance of NOMA-based 5G systems. In this regard, the authors in [22] have derived average bit error rate of the NOMA users over $\alpha - \eta - \mu$ fading channel in terms of H -function. In this study, we examine average bit error rate along with average channel capacity and outage probability of the NOMA users over $\eta - \mu$ fading channel. We present the performance expressions of NOMA users in terms of popular functions which are simpler than H -function and readily available in common simulation softwares. We also compare these observations with a reference system, consisting of genie-based detectors at the users. The genie is assumed to provide every information about the system. Actually, such a genie is unrealistic in the practical sense, but genie-based systems are used to provide reference bounds for different performance metrics of communication systems [23], [24]. It is shown in [25] that side information provided by the genie helps in mitigating unwanted interference. This motivates to compare the derived performance results of the NOMA users with genie-aided NOMA system.

This paper is organized as follows: Section II describes the basic system model used for analyzing the behavior of NOMA users. Section III involves the performance analysis of the downlink NOMA users over $\eta - \mu$ fading channel. Section IV discusses the simulation results followed by conclusion in Section V.

II. SYSTEM MODEL

We consider a downlink system model consisting of a base station (BS) and M users. We assume that perfect channel state information (CSI) is available at the base station. Accordingly, their channel gains are arranged as under [26]

$$|h_1|^2 \geq |h_2|^2 \dots \geq |h_M|^2. \quad (1)$$

It is not practically possible to have all available M users as NOMA users. So, for analysis purpose, we consider only two users, near user m and far user n with $m < n$, transmitting over non-homogenous fading environments [26]. According to NOMA principle, different power levels a_m and a_n are allocated to these two users respectively. We consider that $|h_m|^2 \geq |h_n|^2$, leading to larger fraction of power for user n . This allocation of power between NOMA users is carried out in such a manner that the total available power is equal to unity [27]. Considering these system settings, we analyze the behavior of the NOMA users over $\eta - \mu$ fading channel. This model is used to characterize small-scale fading under NLOS conditions. Over this channel model, the distribution of the

envelope of signal-to-noise ratio (SNR) denoted by γ is given by [28]

$$f_{\eta-\mu}(\gamma) = \frac{2\sqrt{\pi}\mu^{\mu+0.5}h^\mu}{\Gamma(\mu)H^{\mu-0.5}} \frac{\gamma^{\mu-0.5}}{\bar{\gamma}^{\mu+0.5}} \times \exp\left(-2\mu h \frac{\gamma}{\bar{\gamma}}\right) \times I_{\mu-0.5}\left(2\mu H \frac{\gamma}{\bar{\gamma}}\right), \quad (2)$$

where $\mu > 0$ represents the fading parameter and η is defined as the ratio of in-phase power component to quadrature power component. According to the Format-1, the values of H and h are dependent on the values of η such that $H = \frac{\eta^{-1}-\eta}{4}$ and $h = \frac{2+\eta^{-1}+\eta}{4}$. Also, $\Gamma(\cdot)$ is the Gamma function and $I_\nu(\cdot)$ is the modified Bessel function of first kind [28].

III. PERFORMANCE ANALYSIS

A. Average Bit Error Rate (ABER)

We first examine the behavior of average bit error rate of the NOMA users. In case of both the users, the average value of bit error rate (BER) is obtained by evaluating the average of the instantaneous BER over $\eta - \mu$ fading channel.

1) *ABER Analysis of far user n* : The instantaneous bit error rate of the far user n is given by [28, eq. 6]

$$P_n(e) = \frac{1}{2} [Q(\sqrt{\gamma_a}) + Q(\sqrt{\gamma_b})], \quad (3)$$

where $Q(\cdot)$ is Gaussian Q -function. The values of γ_a and γ_b are given by

$$\begin{aligned} \gamma_a &= \left(\sqrt{\frac{2\phi_n}{N_o}} + \sqrt{\frac{\phi_m}{N_o}} \right)^2 |h_n|^2, \\ \gamma_b &= \left(\sqrt{\frac{2\phi_n}{N_o}} - \sqrt{\frac{\phi_m}{N_o}} \right)^2 |h_n|^2, \end{aligned} \quad (4)$$

with ϕ_m and ϕ_n as symbol energies of near user m and far user n respectively. Also, N_o is the power spectral density of additive white Gaussian noise (AWGN) experienced by the NOMA users.

For evaluating average BER over non-homogenous fading channel, we have

$$\overline{P_n(e)} = \frac{1}{2} [I_a + I_b], \quad (5)$$

where

$$I_n = \int_0^\infty Q(\sqrt{\gamma_n}) f_{\gamma_n}(\gamma_n) d\gamma_n, \quad n = a, b. \quad (6)$$

Considering $\eta - \mu$ fading channel, we have

$$\begin{aligned} I_n &= \frac{2\sqrt{\pi}\mu^{\mu+0.5}h^\mu}{\Gamma(\mu)\bar{\gamma}_n^{\mu+0.5}H^{\mu-0.5}} \int_0^\infty Q(\sqrt{\gamma_n}) \gamma_n^{\mu-0.5} \\ &\quad \times \exp\left(-2\mu h \frac{\gamma_n}{\bar{\gamma}_n}\right) I_{\mu-0.5}\left(2\mu H \frac{\gamma_n}{\bar{\gamma}_n}\right) d\gamma_n. \end{aligned} \quad (7)$$

On solving the integral I_n (Appendix A), the respective values of I_a and I_b are inserted in (5), we have

$$\begin{aligned} \overline{P_n(e)} &= \frac{1}{2} \sum_{p=0}^{\infty} \frac{h^\mu H^{2p}}{p!(2\mu+2p)} \frac{\Gamma(2\mu+2p+0.5)}{\Gamma(\mu)\Gamma(\mu+p+0.5)} \\ &\quad \times [F_a + F_b], \end{aligned} \quad (8)$$

where

$$F_n = \left(\frac{2\mu}{\bar{\gamma}_n}\right)^{a'} \times {}_2F_1\left(a', b'; c'; \frac{-4\mu h}{\bar{\gamma}_n}\right), \quad (9)$$

with $n = a, b$ and ${}_2F_1(\cdot, \cdot; \cdot; \cdot)$ denoting Gauss hypergeometric function. The values of a', b', c' are given in Appendix A. In this way, (8) gives the exact closed form average bit error rate of the far user n over $\eta - \mu$ fading channel in terms of Gauss hypergeometric function.

2) *ABER Analysis of near user m* : The instantaneous BER of near user m is given by [28, eq. 18]

$$P_m(e) = \frac{1}{4} [Q(\sqrt{\gamma_c}) \times \{4 - Q(\sqrt{\gamma_d}) - Q(\sqrt{\gamma_e})\} - Q(\sqrt{\gamma_d})], \quad (10)$$

where

$$\begin{aligned} \gamma_c &= \frac{\phi_m}{N_o} |h_m|^2, \quad \gamma_d = \left(\sqrt{\frac{2\phi_n}{N_o}} + \sqrt{\frac{\phi_m}{N_o}}\right)^2 |h_m|^2, \\ \gamma_e &= \left(\sqrt{\frac{2\phi_n}{N_o}} - \sqrt{\frac{\phi_m}{N_o}}\right)^2 |h_m|^2. \end{aligned} \quad (11)$$

For evaluating average BER of near user, we have

$$\overline{P_m(e)} = \frac{1}{4} [I_c \times \{4 - I_d - I_e\} - I_d], \quad (12)$$

where

$$I_m = \int_0^\infty Q(\sqrt{\gamma_m}) f_{\gamma_m}(\gamma_m) d\gamma_m, \quad m = c, d, e. \quad (13)$$

Considering $\eta - \mu$ fading channel, we have

$$\begin{aligned} I_m &= \frac{2\sqrt{\pi}\mu^{\mu+0.5}h^\mu}{\Gamma(\mu)\bar{\gamma}_m^{\mu+0.5}H^{\mu-0.5}} \int_0^\infty Q(\sqrt{\gamma_m}) \gamma_m^{\mu-0.5} \\ &\quad \times \exp\left(-2\mu h \frac{\gamma_m}{\bar{\gamma}_m}\right) I_{\mu-0.5}\left(2\mu H \frac{\gamma_m}{\bar{\gamma}_m}\right) d\gamma_m. \end{aligned} \quad (14)$$

Solving the integral I_m similar to the integral I_n of (7) and upon substituting the obtained values of I_c, I_d and I_e in (12), we have

$$\overline{P_m(e)} = \frac{1}{4} \sum_{p=0}^{\infty} [\tau \cdot F_c \times \{4 - \tau \cdot F_d - \tau \cdot F_e\} - \tau \cdot F_d], \quad (15)$$

where

$$\begin{aligned} \tau &= \frac{h^\mu H^{2p}}{p!(2\mu+2p)} \frac{\Gamma(2\mu+2p+0.5)}{\Gamma(\mu)\Gamma(\mu+p+0.5)}, \\ F_m &= \left(\frac{2\mu}{\bar{\gamma}_m}\right)^{a'} \times {}_2F_1\left(a', b'; c'; \frac{-4\mu h}{\bar{\gamma}_m}\right), \quad m = c, d, e. \end{aligned} \quad (16)$$

So, (16) gives average bit error rate of near user m over $\eta - \mu$ fading channel in terms of Gauss hypergeometric function.

Owing to the wide popularity of Gauss hypergeometric function in deriving most of the physical quantities of a wireless communication system, our derived expressions are quite versatile. Such representation ensures easy implementation in common softwares like MATLAB and Mathematica. Moreover, recent research is tending to improve the computational efficiency of the hypergeometric function [30]. Such approach enhances the popularity of these functions in wireless communication.

B. Average Channel Capacity

Here, we analyze the effect of non-homogenous fading parameters on the maximum achievable capacity of the NOMA users.

1) *Average Channel Capacity of Near User m* : Assuming $y = |h_m|^2$ and ρ as transmit power, the maximum achievable average channel capacity over a general fading channel is given as under [31]

$$\begin{aligned} \overline{C_m} &= \int_0^\infty \log_2(1 + a_m \rho y) f_Y(y) dy, \\ &= \frac{1}{\ln 2} \int_0^\infty \ln(1 + a_m \rho y) f_Y(y) dy. \end{aligned} \quad (17)$$

Rewriting (17) in terms of Meijer G -function, we have

$$\overline{C_m} = \frac{1}{\ln 2} \int_0^\infty G_{2,2}^{1,2}\left(a_m \rho y \middle| \begin{matrix} 1, 1 \\ 1, 0 \end{matrix}\right) f_Y(y) dy. \quad (18)$$

On solving (18) for $\eta - \mu$ fading channel (Appendix B), we obtain the average channel capacity of near user given by

$$\begin{aligned} \overline{C_m} &= \sum_{p=0}^{\infty} \frac{2\sqrt{\pi}}{\ln(2) p! \Gamma(\mu) \Gamma(\mu+p+0.5)} \times \frac{H^{2p}}{2^{2\mu+2p} h^{\mu+2p}} \\ &\quad \times G_{3,2}^{1,3}\left(\frac{a_m \rho \bar{y}}{2\mu h} \middle| \begin{matrix} 1-2\mu-2p, 1, 1 \\ 1, 0 \end{matrix}\right). \end{aligned} \quad (19)$$

So, (19) gives simplified exact closed form expression for average channel capacity of near user over $\eta - \mu$ fading channel in terms of Meijer G -function.

2) *Average Channel Capacity of Far User n* : Assuming $x = |h_n|^2$, the maximum achievable capacity of far user n is given by [31]

$$\overline{C_n} = \frac{1}{\ln 2} \int_0^\infty \ln\left(1 + \frac{a_n \rho x}{a_m \rho x + 1}\right) f_X(x) dx. \quad (20)$$

After algebraic manipulation, we have

$$\overline{C_n} = \frac{1}{\ln 2} \times [C_{n1} - C_{n2}] f_X(x) dx, \quad (21)$$

where

$$\begin{aligned} C_{n1} &= \int_0^\infty \ln(1 + \rho x) f_X(x) dx, \\ C_{n2} &= \int_0^\infty \ln(1 + a_m \rho x) f_X(x) dx. \end{aligned} \quad (22)$$

Solving each integral of (22) for $\eta - \mu$ fading channel using the same procedure similar to (18), we obtain

$$\overline{C_n} = \sum_{p=0}^{\infty} \epsilon \times [G_1 - G_2], \quad (23)$$

where

$$\begin{aligned} \epsilon &= \frac{2\sqrt{\pi}}{\ln(2) p! \Gamma(\mu) \Gamma(\mu+p+0.5)} \times \frac{H^{2p}}{2^{2\mu+2p} h^{\mu+2p}}, \\ G_1 &= G_{3,2}^{1,3}\left(\frac{\rho \bar{x}}{2\mu h} \middle| \begin{matrix} 1-2\mu-2p, 1, 1 \\ 1, 0 \end{matrix}\right), \\ G_2 &= G_{3,2}^{1,3}\left(\frac{a_m \rho \bar{x}}{2\mu h} \middle| \begin{matrix} 1-2\mu-2p, 1, 1 \\ 1, 0 \end{matrix}\right). \end{aligned} \quad (24)$$

In this way, we derive the average channel capacity of far user in terms of Meijer G -function. This function is widely

used in wireless communication and other fields. It has a property that all the special functions can be represented in terms of Meijer G -function [32].

C. Outage Probability

This parameter is helpful in analyzing the performance of the users for different SNR values. This analysis is carried out by considering fixed power allocation strategy.

1) *Outage Probability of Far User n* : We consider an event of having lower data rate than OMA. So, the probability of such an event in case of far user n is given by [32, eq. 7]

$$\begin{aligned} P_n^o &= P \left(\log_2 \left(1 + \frac{a_n |h_n|^2}{a_m |h_n|^2 + \frac{1}{\rho}} \right) < \frac{1}{2} \log_2 (1 + \rho |h_n|^2) \right) \\ &= P \left(|h_n|^2 > \frac{R}{\rho} \right), \end{aligned} \quad (25)$$

where ρ is the transmit SNR and R is given by

$$R = \frac{1 - 2a_m}{a_m^2}. \quad (26)$$

Considering $x = |h_n|^2$ and solving for $\eta - \mu$ fading channel (Appendix C), we have

$$\begin{aligned} P_n^o &= \sum_{i=0}^{M-n} \alpha' \times \binom{M-n}{i} (-1)^i \\ &\times \left[1 - \left\{ 1 - Y_\mu \left(\frac{H}{h}, \sqrt{\frac{2\mu h R}{\bar{x}\rho}} \right) \right\}^{n+i} \right], \end{aligned} \quad (27)$$

with $\alpha' = \frac{M!}{(n-1)!(M-n)!(n+i)}$ and $Y_\mu(\cdot, \cdot)$ denotes Yacoub integral [34]. One problem while implementing (27) is that common software packages lack any function for computing Yacoub integral. One solution is to use its approximation formulas but such an approach leads to an approximate analysis of outage [34]. Considering the exact analysis in terms of simple functions, we exploit different forms of Yacoub integral which are easily implementable in common softwares. Therefore, invoking [35], we rewrite (27) as

$$\begin{aligned} P_n^o &= \sum_{i=0}^{M-n} \alpha' \times \binom{M-n}{i} (-1)^i \\ &\times \left[1 - \left\{ \xi \times \Phi_2(\mu; \mu; 1 + 2\mu, w, z) \right\}^{n+i} \right], \end{aligned} \quad (28)$$

where

$$\begin{aligned} \xi &= \frac{\left(1 - \frac{H^2}{h^2}\right)^\mu \left(\frac{2\mu h R}{\bar{x}\rho}\right)^{2\mu}}{\Gamma(1 + 2\mu)}, \\ w &= -\left(1 + \frac{H}{h}\right) \left(\frac{2\mu h R}{\bar{x}\rho}\right), \\ z &= -\left(1 - \frac{H}{h}\right) \left(\frac{2\mu h R}{\bar{x}\rho}\right), \end{aligned} \quad (29)$$

and $\Phi_2(\cdot; \cdot; \cdot, \cdot, \cdot, \cdot)$ is confluent hypergeometric function, also known as Humbert function [35]. This Humbert function

has a property that it can be expressed in terms of Gauss hypergeometric function. So, using [35, eq. 1.11], we have

$$\begin{aligned} P_n^o &= \sum_{i=0}^{M-n} \alpha' \times \binom{M-n}{i} (-1)^i \\ &\times \left[1 - \left\{ \xi' \times \sum_{k=0}^{\infty} {}_2F_1 \left(-k, \mu; 1 - \mu - k; \frac{z}{w} \right) \frac{w^k}{k!} \right\}^{n+i} \right], \end{aligned} \quad (30)$$

with $\xi' = \xi \times (\mu)_k / (1 + 2\mu)_k$ and $(\cdot)_k$ denotes Pochhammer symbol.

In this way, (30) represents the expression of outage probability of far user n over $\eta - \mu$ fading in terms of Gauss hypergeometric function.

2) *Outage Probability of Near User m* : In order to evaluate the OP of near user m , we consider that near user m obtains its own original message after decoding and subtracting the message signal of far user from the received signal. So, assuming R_n as the target rate of user m , the probability that user m shows lesser performance in NOMA than OMA is given by [32, eq. 23]

$$\begin{aligned} P_m^{out} &= P \left(\log_2 \left(1 + \frac{a_n |h_m|^2}{a_m |h_m|^2 + \frac{1}{\rho}} \right) < R_n \right) \\ &+ P \left(\log_2 \left(1 + \frac{a_n |h_m|^2}{a_m |h_m|^2 + \frac{1}{\rho}} \right) > R_n, \right. \\ &\left. \log_2 (1 + a_m \rho |h_m|^2) < \frac{1}{2} \log_2 (1 + \rho |h_m|^2) \right), \\ P_m^o &= P \left(|h_m|^2 < \frac{R}{\rho} \right). \end{aligned} \quad (31)$$

Assuming $y = |h_m|^2$ and solving similar to (25), we have

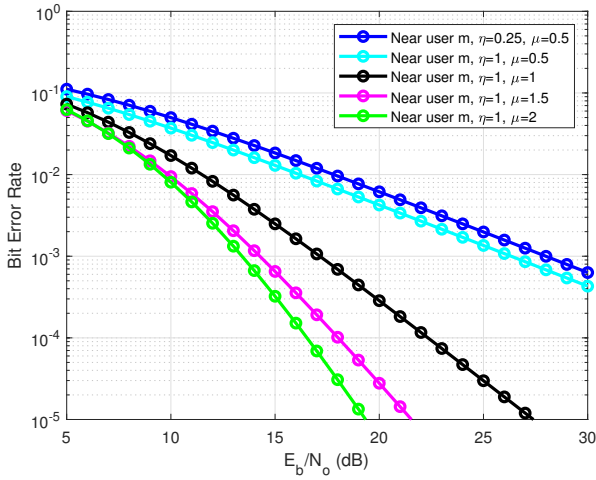
$$\begin{aligned} P_m^o &= \sum_{i=0}^{M-m} \beta' \times \binom{M-m}{i} (-1)^i \\ &\times \left[1 - Y_\mu \left(\frac{H}{h}, \sqrt{\frac{2\mu h R}{\bar{y}\rho}} \right) \right]^{m+i}, \end{aligned} \quad (32)$$

with $\beta' = \frac{M!}{(m-1)!(M-m)!(m+i)}$. Similar to the case of far user n , we also represent the OP of near user m in terms of Gauss hypergeometric function. So, we have

$$\begin{aligned} P_m^o &= \sum_{i=0}^{M-m} \beta' \times \binom{M-m}{i} (-1)^i \\ &\times \left[\zeta' \times \sum_{k=0}^{\infty} {}_2F_1 \left(-k, \mu; 1 - \mu - k; \frac{v}{u} \right) \frac{u^k}{k!} \right]^{m+i} \end{aligned} \quad (33)$$

where

$$\begin{aligned} \zeta' &= \frac{\left(1 - \frac{H^2}{h^2}\right)^\mu \left(\frac{2\mu h R}{\bar{y}\rho}\right)^{2\mu}}{\Gamma(1 + 2\mu)} \times \frac{(\mu)_k}{(1 + 2\mu)_k}, \\ u &= -\left(1 + \frac{H}{h}\right) \left(\frac{2\mu h R}{\bar{y}\rho}\right), \\ v &= -\left(1 - \frac{H}{h}\right) \left(\frac{2\mu h R}{\bar{y}\rho}\right). \end{aligned} \quad (34)$$

Fig. 1. Average BER performance of near user m

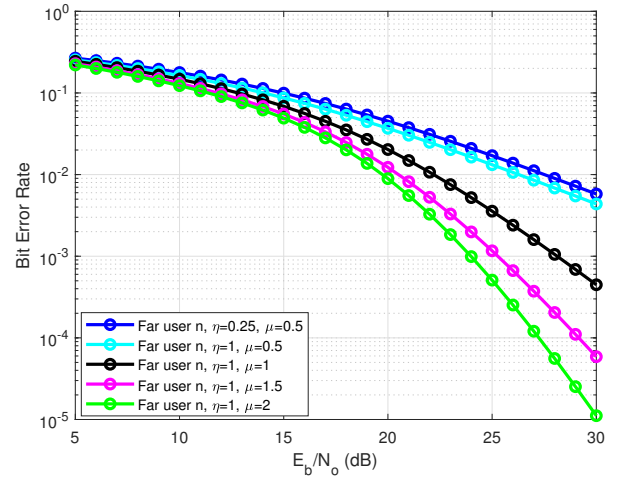
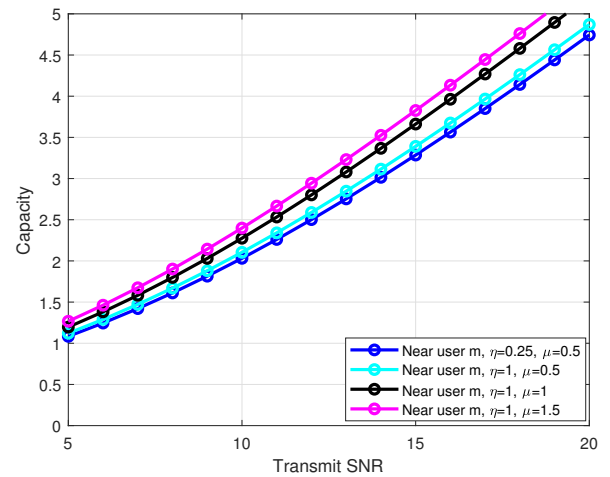
In this study, all the derived OP expressions are compact and tractable. These equations are presented in terms of Gauss hypergeometric function, which is the most convenient form. Such an approach helps in the easy implementation of these derived expressions.

IV. RESULTS AND DISCUSSIONS

We simulate the downlink NOMA model given in Section II and observe the behavior of NOMA users over diverse fading channels modeled by taking different values of parameters η and μ . For simulation, we consider $M = 5$, $m = 2$, $n = 3$ [33]. We assume the power coefficients $a_m = 0.2$ and $a_n = 0.8$ for near user m and far user n respectively. Under such system settings, we simulate the average bit error rate, average channel capacity and outage probability curves of the NOMA users and observe the impact of the parameters η and μ on these metrics. We also interpret the obtained results in relation to the genie-aided NOMA system. In the obtained graphs, the line markers (-o) represent simulation results which closely match with the derived analytical results represented by solid lines.

A. Average bit error rate

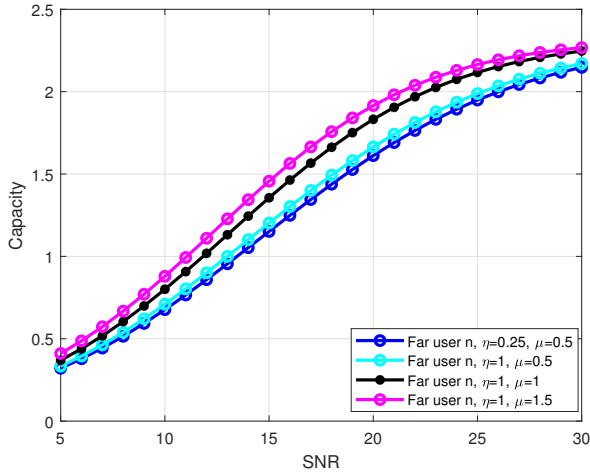
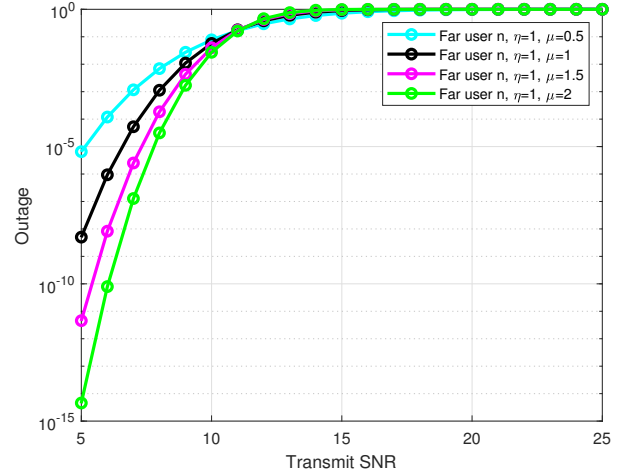
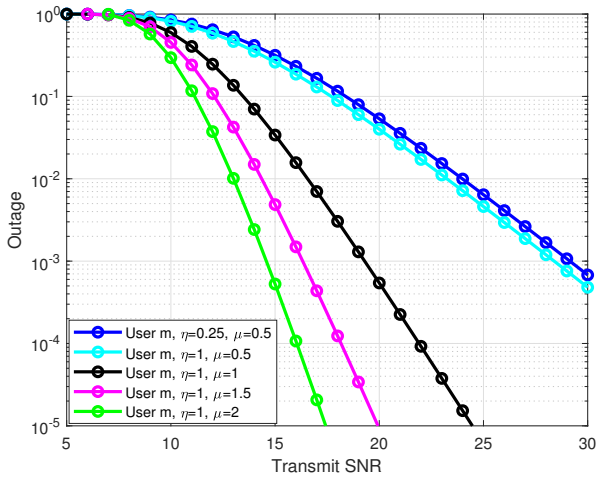
The ABER performance results of both the NOMA users are shown in Fig. 1 and Fig. 2. For simulation, we consider different values of parameters η and μ leading to special fading scenarios. From the graph curves, it is clear that in each case, BER curve decreases with an increase in SNR leading to a waterfall type curve. This behavior of NOMA users is validated by the usual behavior shown by BER with the increase in SNR [37]. We also observe that considering the parameter η constant and increasing the value of parameter μ leads to improved BER performance. This is due to the fact that a higher value of parameter μ means lesser amount of fading and thus, leads to better ABER. Also, on increasing the value of parameter η with parameter μ as constant causes slight decrease in BER. Such play around the values of parameters η and μ reveals that the impact of parameter μ on ABER is more significant than parameter η .

Fig. 2. Average BER performance of far user n Fig. 3. Average channel capacity performance of near user m

B. Average Channel Capacity

The average channel capacity performance of near user m over $\eta - \mu$ fading channel is given in Fig. 3. Here, we consider different values of parameters η and μ for near user m and corresponding curves leading to different fading scenarios are shown. We observe that each capacity curve increases with increase in transmit SNR. It is also clear from the curves that as we increase the value of parameter μ , the effect of fading on the achievable capacity decreases making the average capacity to increase.

Further, the average channel capacity curves of far user n over $\eta - \mu$ fading for different values of parameters η and μ are given in Fig. 4. We observe that each capacity curve initially increases with an increase in SNR. However, at high SNR, the capacity saturates due to interference from near user m . Moreover, we consider different values of parameter μ and observe that increasing the value of parameter μ leads to improved capacity. Also, the impact of increasing the parameter η on the achieved channel capacity is less significant

Fig. 4. Average channel capacity performance of far user n Fig. 6. Outage probability performance of far user n Fig. 5. Outage probability performance of near user m

than the impact of increasing the parameter μ .

C. Outage Probability

For the near user m , the OP curves are shown in Fig. 5. We observe that each OP curve shows decrease in outage with increase in SNR. Moreover, by increasing the value of parameter μ and keeping the value of parameter η constant, there is decrease in outage. This is attributed to the fact that higher value of parameter μ means lesser degree of fading and hence, lesser outage. Further, on increasing the value of parameter η and keeping μ constant, the OP performance is slightly improved.

For far user n , the OP curves over $\eta - \mu$ fading channel are presented in Fig. 6. We observe that each OP curve of far user n increases with increase in transmit SNR and saturates to a constant value at high SNR. Such constant outage at high SNR is a challenging issue in case of far user. Also, on increasing the value of parameter μ , the effect of fading decreases on outage leading to better performance.

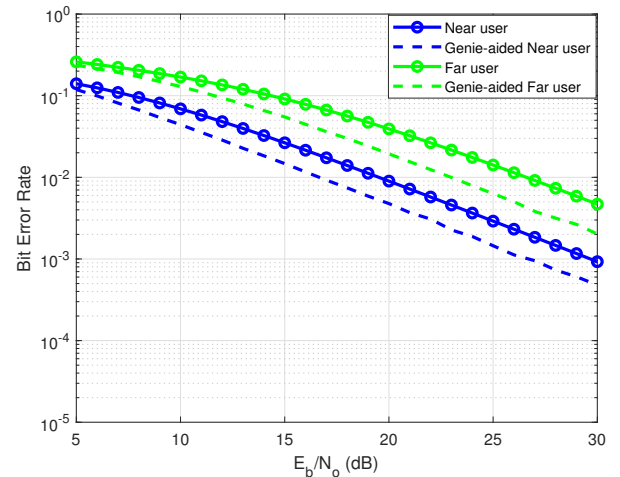


Fig. 7. ABER comparison with genie-aided NOMA system

There is a disparity in the behavior of OP and ACC curves of near user m and far user n with increase in SNR. Significantly, far user n shows crucial behavior at high SNR. Such observations match with the remarks drawn in [33] over Nakagami- m fading channel which validate the findings of this paper.

D. Comparison with Genie-aided NOMA System

We simulate genie-aided NOMA system wherein genie assists the users by providing accurate information about the channel coefficients and interference signals. Considering this set up as a reference system, we assume Rayleigh channel ($\eta = 1$, $\mu = 0.5$) and compare the obtained results of both unaided and genie-aided NOMA users as shown in Fig. 7, Fig. 8 and Fig. 9.

We observe that genie-aided system leads to better BER performance than unaided NOMA users. So, we interpret that the ideal genie in NOMA system provides a lower bound of BER performance for both the users given in Fig. 7.

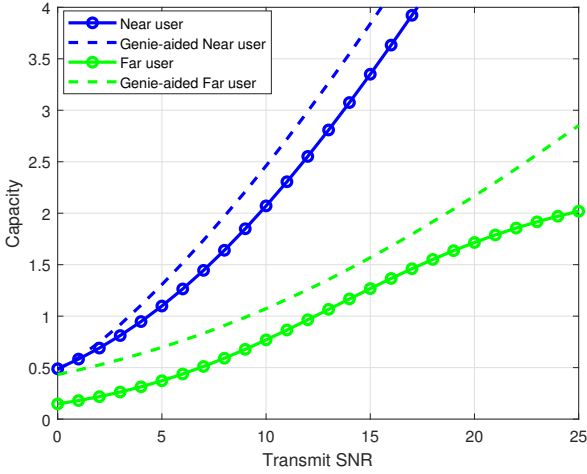


Fig. 8. ACC comparison with genie-aided NOMA system

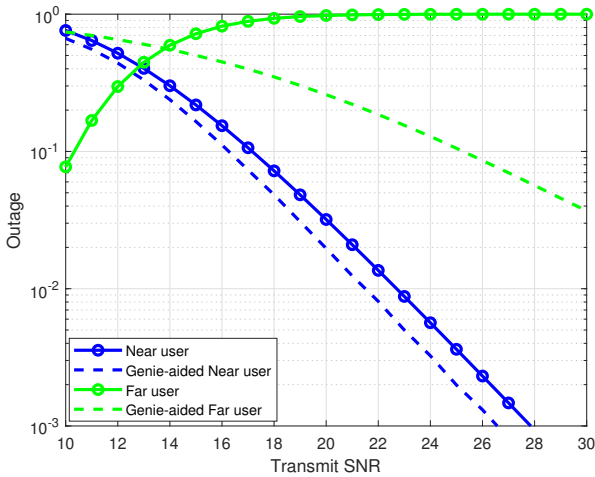


Fig. 9. OP comparison with genie-aided NOMA system

In case of channel capacity, genie-aided NOMA users show better performance. So, an upper bound for achievable capacity is obtained using genie. Moreover, the genie-aided far user is able to mitigate the interference from near user leading to negligible saturation at high SNR as shown in Fig. 8.

For outage probability, genie helps in decreasing the outage of the NOMA users with increase in SNR. So, genie-aided NOMA system also provides lower bound of outage performance for the users as shown in Fig. 9. The unaided far user suffers from the interference of near user which leads to increase in outage with increase in SNR. But, genie helps far user in overcoming the effect of interference leading to decrease in outage with increase in SNR.

V. CONCLUSION

NOMA has a tendency to cater the incessant demands of the increasing number of users. In this paper, we explore the behavior of NOMA users over the most realistic environment conditions for 5G transmission. For modeling such environment, we consider $\eta - \mu$ fading channel. We derive

unified exact expressions of average bit error rate (ABER), average channel capacity (ACC) and outage probability (OP) of both the users in terms of Gauss hypergeometric function and Meijer G -function. This approach overcomes the issue of expressing the outage probability expressions in terms of Yacoub integral. We examine the impact of the parameters η and μ on these performance metrics. We observe that increasing the value of parameter μ leads to prominent improvement in ABER, ACC and OP of both the NOMA users. Such improvement is attributed to the fact that higher value of parameter μ means lower amount of fading which increases the overall performance of the system. Further, increasing the value of parameter η and keeping parameter μ constant also leads to improvement in the metrics of the NOMA users. However, the impact of increasing the parameter η is less significant than the impact of increasing the parameter μ . Moreover, the ABER behaviors of the users reflect one common trend which is the decrease in average error rate with increasing SNR. Although, the ACC and OP curves of the near and far user reveal different trends respectively. In case of near user, ACC curves show increase in capacity with increase in SNR, while the capacity curve saturates at high SNR in case of far user. Furthermore, the OP decreases with increasing SNR for near user. Instead of this, the OP of far user increases and saturates at high SNR. Such behavior at high SNR poses challenges for the NOMA system. We also compare the obtained results with genie-aided NOMA system. We interpret that genie-aided system acts as a reference system to provide performance bounds for both the unaided NOMA users. We observe that genie presents lower bounds for ABER and OP performance, along with upper bound for ACC. For confirming these observations, simulations are carried out which corroborate the derived analytical results. As a future extension of this work, we propose to present the compact and simpler expressions of the performance metrics of the NOMA users under imperfect channel state information and other practical impairments.

APPENDIX A

We consider $\gamma_n = z^2$ and express the Gaussian Q -function in terms of complementary Gaussian error function in (7). Along with this, we also substitute the Taylor series expansion of modified Bessel's function of first kind $I_\nu(\cdot)$ [37, eq. 8.445] in (7). So, we have

$$I_n = \sum_{p=0}^{\infty} \int_0^{\infty} A \times \operatorname{erfc}\left(\frac{z}{\sqrt{2}}\right) z^{4\mu+4p-1} \times \exp\left(\frac{-2\mu h}{\bar{\gamma}_n} z^2\right) dz, \quad (35)$$

where

$$A = \frac{2\sqrt{\pi}\mu^{\mu+0.5} h^\mu}{\Gamma(\mu)\bar{\gamma}_n^{\mu+0.5} H^{\mu-0.5}} \times \frac{\left(\frac{\mu h}{\bar{\gamma}_n}\right)^{\mu-0.5+2p}}{p! \Gamma(\mu+p+0.5)}. \quad (36)$$

On comparing (35) with [38, 4.3.9], we have

$$I_n = \sum_{p=0}^{\infty} \frac{h^\mu H^{2p}}{p!(2\mu+2p)} \frac{\Gamma(2\mu+2p+0.5)}{\Gamma(\mu+p+0.5)} \left(\frac{2\mu}{\bar{\gamma}_n}\right) \times {}_2F_1\left(a, b; c; \frac{-4\mu h}{\bar{\gamma}_n}\right), \quad (37)$$

with

$$a' = 2\mu + 2p, \quad b' = 2\mu + 2p + 0.5, \quad c' = 2\mu + 2p + 1. \quad (38)$$

For $n = a, b$ in (37), we obtain the respective values of the integrals I_a & I_b .

APPENDIX B

For $\eta - \mu$ fading distribution, (18) is solved as under

$$\bar{C}_m = B \times \int_0^\infty G_{2,2}^{1,2} \left(a_m \rho y \left| \begin{matrix} 1, 1 \\ 1, 0 \end{matrix} \right. \right) y^{\mu-0.5} \times \exp\left(-2\mu h \frac{y}{\bar{\gamma}}\right) I_{\mu-0.5} \left(2\mu H \frac{y}{\bar{\gamma}} \right) dy, \quad (39)$$

where

$$B = \frac{2\sqrt{\pi}\mu^{\mu+0.5} h^\mu}{\ln(2) \Gamma(\mu) \bar{\gamma}^{\mu+0.5} H^{\mu-0.5}}. \quad (40)$$

With the aid of [37, eq. 8.445] in (39), we have

$$\bar{C}_m = \sum_{p=0}^{\infty} B' \times \int_0^\infty G_{2,2}^{1,2} \left(a_m \rho y \left| \begin{matrix} 1, 1 \\ 1, 0 \end{matrix} \right. \right) \times y^{2\mu+2p-1} \times \exp\left(-2\mu h \frac{y}{\bar{\gamma}}\right) dy, \quad (41)$$

where

$$B' = B \times \frac{\left(\frac{\mu h}{\bar{\gamma}}\right)^{\mu+2p-0.5}}{p! \Gamma(\mu+p+0.5)}. \quad (42)$$

Upon comparing (41) with [37, 7.813], we obtain the final expression of \bar{C}_m .

APPENDIX C

Using the marginal PDF of x [40] in (25), we have

$$P_n^o = P\left(|h_n|^2 > \frac{R}{\rho}\right), \\ = \int_{\frac{R}{\rho}}^\infty \alpha \times f(x) [F(x)]^{n-1} [1 - F(x)]^{M-n} dx, \quad (43)$$

where

$$\alpha = \frac{M!}{(n-1)!(M-n)!}. \quad (44)$$

On solving and using binomial expansion, we have

$$P_n^o = \sum_{i=0}^{M-n} \alpha' \binom{M-n}{i} (-1)^i \times \left(1 - F\left(\frac{R}{\rho}\right)^{n+i}\right), \quad (45)$$

where $\alpha' = \frac{\alpha}{(n+i)}$ and $F\left(\frac{R}{\rho}\right)$ is cumulative distribution function (CDF) of $|h_n|^2$.

Substituting CDF expression of $\eta - \mu$ fading channel [41] in (45), we obtain the outage probability expression of far user.

REFERENCES

- [1] M. Hussain, H. Rasheed, "Non-orthogonal multiple access for Next-generation mobile networks: A technical aspect for research direction", *Wireless Communications and Mobile Computing*, 2020, doi: 10.1155/2020/8845371.
- [2] M. Aldababsa, M. Toka, S. Gökçeli, G.K. Kurt, O. Kucur, "A tutorial on Non-orthogonal multiple access for 5G and beyond," *Wireless Communications and Mobile Computing, Hindawi Publications*, 2018, doi: 10.1155/2018/9713450.
- [3] S. M. R. Islam, N. Avazov, O. A. Dobre, K. Kwak, "Power-domain Non-orthogonal multiple access (NOMA) in 5G systems: Potentials and challenges," *IEEE Communications Surveys and Tutorials*, vol. 19, no. 2, pp. 721-742, 2016, doi:10.1109/COMST.2016.2621116.
- [4] M. Vaezi, G. A. Aruma Baduge, Y. Liu, A. Arafa, F. Fang, Z. Ding, "Interplay between NOMA and other emerging technologies: A survey," *IEEE Transactions on Cognitive Communications and Networking*, vol. 5, no. 4, pp. 900-919, Dec. 2019, doi: 10.1109/TCCN.2019.2933835.
- [5] A. Anwar, B.C. Seet, M.A. Hasan, X.J. Li, "A survey on application of non-orthogonal multiple access to different wireless networks," *Electronics*, 8, 1355, 2019, doi: 10.3390/electronics8111355.
- [6] H. Mathur, T. Deepa, "A survey on advanced multiple access techniques for 5G and beyond wireless communications," *Wireless Personal Communications*, 118(2):1775-92, 2021, doi: 10.1007/s11277-021-08115-w.
- [7] H. Lee, S. Kim, J. Lim, "Multiuser superposition transmission (MUST) for LTE-A systems," *IEEE International Conference on Communications (ICC)*, pp. 1-6, 2016, doi: 10.1109/ICC.2016.7510909.
- [8] V.K. Trivedi, K. Ramadan, P. Kumar, M.I. Dessouky, F.E. Abd El-Samie, "Enhanced OFDM-NOMA for Next generation wireless communication: A study of PAPR reduction and sensitivity to CFO and estimation errors," *AEU-International Journal of Electronics and Communications*, 102:9-24, 2019, doi:10.1016/j.aeue.2019.01.009.
- [9] S. Mukhtar, G.R. Begh, "Performance analysis of Filtered OFDM based downlink and uplink NOMA System over Nakagami- m fading channel," *Journal of Telecommunications and Information Technology*, 1(2):11-23, 2021, doi: 10.26636/jtit.2021.148020.
- [10] Y. Zhang, H. Wang, T. Zheng, Q. Yang, "Energy-efficient transmission design in Non-orthogonal multiple access," *IEEE Transactions on Vehicular Technology*, vol. 66, no. 3, pp. 2852-2857, 2017, doi: 10.1109/TVT.2016.2578949.
- [11] Z. Ding, Z. Yang, P. Fan, H. V. Poor, "On the performance of Non-orthogonal multiple access in 5G systems with randomly deployed users," *IEEE Signal Processing Letters*, vol. 21, no. 12, pp. 1501-1505, 2014, doi: 10.1109/LSP.2014.2343971.
- [12] J. Choi, "NOMA-based random access with multichannel ALOHA," *IEEE Journal on Selected Areas in Communications*, vol. 35, no. 12, pp. 2736-2743, 2017, doi: 10.1109/JSAC.2017.2766778.
- [13] X. Shao, Z. Sun, M. Yang, S. Gu, Q. Guo, "NOMA-based irregular repetition slotted ALOHA for satellite networks," *IEEE Communications Letters*, vol. 23, no. 4, pp. 624-627, 2019, doi: 10.1109/LCOMM.2019.2900319.
- [14] F. Babich, G. Buttazzoni, F. Vatta, M. Comisso, "Energy-constrained NOMA with packet diversity for slotted Aloha systems," *Mediterranean Communication and Computer Networking Conference (MedComNet)*, pp. 1-8, 2020, doi: 10.1109/MedComNet49392.2020.9191488.
- [15] X. Yan, H. Xiao, C. Wang, K. An, "Outage performance of NOMA-based hybrid satellite-terrestrial relay networks," *IEEE Wireless Communications Letters*, vol. 7, no. 4, pp. 538-541, 2018, doi: 10.1109/LWC.2018.2793916.
- [16] X. Yue, Y. Liu, Y. Yao, T. Li, X. Li, R. Liu, A. Nallanathan, "Outage behaviors of NOMA-based satellite network over shadowed Rician fading channel," *IEEE Transactions on Vehicular Technology*, vol. 69, no. 6, pp. 6818-6821, 2020, doi: 10.1109/TVT.2020.2988026.
- [17] Z. Gao, A. Liu, C. Han, X. Liang, "Sum rate maximization of Massive MIMO NOMA in LEO satellite communication system," *IEEE Wireless Communications Letters*, 2021, doi: 10.1109/LWC.2021.3076579.
- [18] V. Singh, P. K. Upadhyay, M. Lin, "On the performance of NOMA-assisted overlay multiuser cognitive satellite-terrestrial networks," *IEEE Wireless Communications Letters*, vol. 9, no. 5, pp. 638-642, 2020, doi: 10.1109/LWC.2020.2963981.
- [19] T. Ernest, A. Madhukumar, R. Sirigina, A. Krishna, "NOMA-aided UAV communications over correlated Rician shadowed fading channels," *IEEE Transactions on Signal Processing*, vol. 68, pp. 3103-3116, 2020, doi: 10.1109/TSP.2020.2994781.
- [20] M. Jain, N. Sharma, A. Gupta, D. Rawal, P. Garg, "Performance analysis of NOMA assisted underwater visible light communication System,"

IEEE Wireless Communications Letters, vol. 9, no. 8, pp. 1291-1294, 2020, doi: 10.1109/LWC.2020.2988887.

- [21] M. D. Yacoub, "The $\kappa - \mu$ distribution and the $\eta - \mu$ distribution," *IEEE Antennas and Propagation Magazine*, vol. 49, no. 1, pp. 68-81, 2007, doi: 10.1109/MAP.2007.370983.
- [22] A. S. Alqahtani, E. Alsusa, "Performance analysis of downlink NOMA system over $\alpha - \eta - \mu$ generalized fading channel," *IEEE 91st Vehicular Technology Conference (VTC2020-Spring)*, pp. 1-5, 2020, doi: 10.1109/VTC2020-Spring48590.2020.9128419.
- [23] H.B. Eriksson, P. Odling, T. Koski, P.O. Borjesson, "A genie-aided detector with a probabilistic description of the side information," *Proceedings of 1995 IEEE International Symposium on Information Theory*, pp. 332, 1995, doi: 10.1109/ISIT.1995.550319.
- [24] I. Khan, J.J. Rodrigues, J. Al-Muhtadi, M.I. Khattak, Y. Khan, F. Altaf, S.S. Mirjavadi, B.J. Choi, "A robust channel estimation scheme for 5G massive MIMO systems," *Wireless Communications and Mobile Computing*, 2019, doi: 10.1155/2019/3469413.
- [25] R.H. Etkin, D.N.C. Tse, H. Wang, "Gaussian Interference Channel Capacity to Within One Bit," *IEEE Transactions on Information Theory*, vol. 54, no. 12, pp. 5534-5562, 2008, doi: 10.1109/TIT.2008.2006447.
- [26] Z. Ding, P. Fan, H.V. Poor, "Impact of user pairing on 5G Non-orthogonal multiple access downlink transmissions," *IEEE Transactions on Vehicular Technology*, vol. 65, no. 8, pp. 6010-6023, 2015, doi:10.1109/TVT.2015.2480766.
- [27] M. Jain, S. Soni, N. Sharma, D. Rawal, "Performance analysis at far and near user in NOMA based system in presence of SIC error," *AEU - International Journal of Electronics and Communications*, Volume 114, 2020, doi: 10.1016/j.aeue.2019.152993.
- [28] B. Kumbhani, R.S. Kshetrimayum, "MIMO wireless communications over generalized fading channels," *CRC Press*, 2017, doi: 10.1201/9781315116778.
- [29] K. Ferdi, H. Kaya, "BER performances of downlink and uplink NOMA in the presence of SIC errors over fading channels", *IET Communications*, 2018, 1834-1844, doi:10.1049/iet-com.2018.5278.
- [30] J. Cai, M. Chen, S. Zhang, C. Hong and Y. Lu, "A Fast Algorithm for Solving a Kind of Gauss Hypergeometric Functions in Wireless Communication Based on Pfaff Transformation", *2019 International Conference on Networking and Network Applications, Daegu, Korea (South)*, 2019, pp. 85-89, doi: 10.1109/NaNA.2019.00024.
- [31] B. M. ElHalawany, F. Jameel, D. B. da Costa, U. S. Dias and K. Wu, "Performance Analysis of Downlink NOMA Systems over $\kappa - \mu$ Shadowed Fading Channels", in *IEEE Transactions on Vehicular Technology*, vol. 69, no. 1, pp. 1046-1050, doi:10.1109/TVT.2019.2953109.
- [32] R. Beals R, J. Szmigielski, "Meijer G-functions: a gentle introduction," *Notices of the AMS*, 60(7):866-72, 2013.
- [33] T. Hou, X. Sun, Z. Song, "Outage Performance for Non-orthogonal Multiple Access with Fixed Power Allocation over Nakagami- m Fading Channels," *IEEE Communications Letters*, vol. 22, no. 4, pp. 744-747, 2018, doi: 10.1109/LCOMM.2018.2799609.
- [34] P. Sharma, A. Kumar, M. Bansal, "Performance analysis of downlink NOMA over $\eta - \mu$ and $\kappa - \mu$ fading channels", *IET Communications*, pp:522-531, 2019, doi:10.1049/iet-com.2019.0413.
- [35] D. Morales-Jiménez, J. F. Paris, "Outage probability analysis for $\eta - \mu$ fading channels", *IEEE Communications Letters*, vol. 14, no. 6, pp. 521-523, 2010, doi: 10.1109/LCOMM.2010.06.092501.
- [36] Y.A. Brychkov, Y.S. Kim, A.K. Rathie, "On new reduction formulas for the Humbert functions Ψ_2 , Φ_2 and Φ_3 ", *Integral Transforms and Special Functions*, 350-360, 2017, doi: 10.1080/10652469.2017.1297438.
- [37] M. K. Simon, M.S. Alouini, "Digital Communication Over Fading Channels," *John Wiley & Sons*, 2005.
- [38] I.S. Gradshteyn, I.M. Ryzhik, "Table of integrals, series, and products", *7th edition, San Diego, Academic Press*, 2014.
- [39] E. W. Ng and M. Geller, "A Table of Integrals of the Error Functions", *Journal of Research of the National Bureau of Standards - B. Mathematical Sciences*, Vol. 73B, No. 1.
- [40] H.A. David, H.N. Nagaraja, "Order statistics," *John Wiley & Sons*, 2004, doi: 10.1002/0471667196.ess6023.
- [41] M. D. Yacoub, "The $\eta - \mu$ distribution: a general fading distribution," *52nd IEEE Vehicular Technology Conference Fall*, pp. 872-877 vol.2, 2000, doi: 10.1109/VETECF.2000.887126.



Shaika Mukhtar has done B.E. and M.Tech in Electronics and Communication Engineering in 2012 and 2015 respectively. Currently, she is pursuing Ph.D in National Institute of Technology Srinagar. She is working as Senior Research Fellow in Advanced Communication Lab at NIT Srinagar. Her areas of interest are wireless communication, Non-orthogonal multiple access, High speed Networks and Next generation Networks. Her research aims at understanding the different aspects of NOMA (Non-orthogonal multiple access) for future communication networks. She is a student member of IEEE society.



Gh. Rasool Begh has done Ph.D. from National Institute of Technology Srinagar, Jammu and Kashmir, India. He is working as Associate Professor in the Department of Electronics and Communication Engineering at NIT Srinagar. He has a teaching experience of more than 20 years. He has guided a number of M.Tech. thesis related to OFDM, Cognitive Radios, WLANs and Security. His areas of interest include Cognitive Radios, OFDM, MIMO, Cooperative Communications, D2D communication, Error control coding and Security. He is a member of IEEE MTTS Society.